Two Lead Borate-nitrates with Anion-Centered [OPb_4] Tetrahedra and Two Types of π-Conjugated Planar Units Showing Large Birefringence

Shuo Bai,[a] Daqing Yang,[a] Bingbing Zhang,[a] Ling Li,[b] and Ying Wang*[a]

[a] *College of Chemistry and Environmental Science, Hebei University, Baoding 071002, China. Email: wangy@hbu.edu.cn.*

[b] *College of Physics Science and Technology, Hebei University, Baoding 071002, China.*

Table of contents

Experimental section

Synthesis. All chemicals were used as received without further purification. Single crystals of $Pb_6O_4(BO_3)(NO_3)$ and $Pb_6O_2(BO_3)_2(NO_3)F$ were synthesized by using the high-temperature solution method. For $Pb_6O_4(BO_3)(NO_3)$, the raw materials consist of PbF_2 (0.230 g, 0.9 mmol), $Pb(NO_3)_2$ (2.180 g, 6.6 mmol), Na_2CO_3 (0.299 g, 2.8 mmol), and H_3BO_3 (0.291 g, 4.7 mmol), while PbF_2 (0.313 g, 0.9 mmol), $Pb(NO_3)_2$ (1.3 g, 3.8 mmol), $PbCO_3$ (1.024 g, 3.8 mmol), and H_3BO_3 (0.394 g, 6.4 mmol) were used for the synthesis of $Pb_6O_2(BO_3)_2(NO_3)F$. The raw materials were mixed and grounded and then transferred into alumina crucibles. For $Pb_6O_4(BO_3)(NO_3)$, the temperature was slowly raised to 500 °C and maintained for 6 h, cooled down to 420 °C in 2 h, and subsequently cooled slowly to 320 °C at a rate of 2 $°C·h^{-1}$, finally decreased rapidly to room temperature in 3 h. For $Pb_6O_2(BO_3)_2(NO_3)F$, the temperature was slowly raised to 500 °C and held for 6 h, cooled down to 400 °C at a rate of 2 $°C·h^{-1}$, and subsequently cooled to room temperature in 50 h. Small crystals (~0.1 mm) of the title compounds were obtained from the crushed products.

Polycrystalline samples of the title compounds were prepared by the conventional solid-state method. For $Pb_6O_4(BO_3)(NO_3)$, $Pb(NO_3)_2$, $PbCO_3$, and H_3BO_3 were weighed according to the stoichiometric ratio, and the raw materials were fully grounded before transferring to an alumina crucible with cover. The sample was first heated to 400 °C in a muffle furnace and held at this temperature for 24 h to decompose $PbCO_3$, then kept at 380 °C for 48 h, and finally calcined at 350 °C for 48h with several times mid-grinding. For $Pb_6O_2(BO_3)_2(NO_3)F$, the stoichiometric ratio of PbF_2, $Pb(NO_3)_2$, $PbCO_3$, and H_3BO_3 were ground thoroughly. The mixture was preheated at 300 °C for 24 h, then heated at 350 °C for 24 h and 380 °C for 24 h with intermediate grinding. Yellow polycrystalline powder samples were obtained with high phase purity.

Characterization. The single-crystal X-ray diffraction (XRD) data were collected on a Bruker D8 VENTURE diffractometer equipped with a PHOTON II detector and Mo IμS 3.0 microfocus X-ray sources (λ = 0.71073 Å). Data integration and absorption corrections were carried out using the *SAINT* program.[1] The structure solution and refinement were performed using the Intrinsic Phasing method and the least-squares technique, respectively, embedding within the *Olex*2 program.[2] Crystal data and refinement details, atomic coordinates, and selected bond distances and angles are listed in Tables S1-S3. Powder XRD data were measured on a Dandong Haoyuan DX-27mini X-ray diffractometer with Cu Kα radiation (λ = 1.54056 Å). The powder XRD pattern was scanned over the 2θ angles range of 5-70°, at a scanning step width of 0.02° and a fixed counting time of 2 s. The thermal gravimetric (TG) analysis and differential scanning calorimetry (DSC) were studied with a NETZSCH5 instrument under air. The sample was placed in an Al_2O_3 crucible and heated from 30 to 800 °C with a heating rate of 10 $°C·min^{-1}$. The infrared spectra were recorded on a Shimadzu IR Affinity-1 Fourier transform infrared spectrometer in the range of 400 - 4000 cm^{-1}. The sample was grounded and mixed with KBr. The UV−Vis−NIR diffuse reflectance spectra were measured at room temperature with a Shimadzu SolidSpec-3600DUV spectrophotometer in the 200–1100 nm wavelength range.

Theoretical Calculations. The electronic structures and optical properties for $Pb_6O_4(BO_3)(NO_3)$ and $Pb_6O_2(BO_3)_2(NO_3)F$ were calculated by using the CASTEP package.[3] The generalized gradient-approximation (GGA) with Perdew-Burke-Ernzerhof (PBE) functional was selected as exchange-correlation potential.[4] The norm-conserving pseudopotentials (NCP) were adopted to model the effective interaction between the valence electrons and atom cores.[5] The cut off energies and the dense *K*-points in the Brillouin zone were set as 820 eV and 2 × 2 × 1 for $Pb_6O_4(BO_3)(NO_3)$, and 850 eV and 2 × 1 × 2 for $Pb_6O_2(BO_3)_2(NO_3)F$. The configurations for diverse electron orbital were Pb: $5s^25p^65d^{10}6s^26p^2$, B: $2s^22p^1$, N: $2s^22p^3$, O: $2s^22p^4$, and F: $2s^22p^5$, respectively.

Table S1. Crystal data and structure refinements for $Pb_6O_4(BO_3)(NO_3)$ and $Pb_6O_2(BO_3)_2(NO_3)F$.

Compound	$Pb_6O_4(BO_3)(NO_3)$	$Pb_6O_2(BO_3)_2(NO_3)F$
Formula weight	1427.96	1473.77
Temperature (K)	273.15	
Wavelength (Å)	0.71073	
Crystal system, space group	Orthorhombic, *Pmmn*	Monoclinic, $P2_1/m$
a (Å)	5.7481(5)	6.8025(7)
b (Å)	9.4582(9)	11.5092(9)
c (Å)	11.2770(12)	8.8989(9)
β (deg)		101.704(4)
Volume (Å^3)	613.09(10)	682.22(11)
Z, Calculated density (g·cm^{-3})	2, 7.735	2, 7.174
Absorption coefficient (mm^{-1})	82.125	73.830
F(000)	1168	1212
Theta range for data collection (deg.)	2.811 to 27.530	2.337 to 27.509
Limiting indices	$-7 \le h \le 7$, $-12 \le k \le 12$, $-14 \le l \le 14$	$-8 \le h \le 8$, $-14 \le k \le 14$, $-11 \le l \le 11$
Reflections collected / unique	6656 / 823 [R(int) = 0.0664]	19582 / 1645 [R(int) = 0.0663]
Completeness	98.9 %	100.0 %
Max. and min. transmission	0.0206 and 0.0040	0.0481 and 0.0007
Data / restraints / parameters	823 / 0 / 58	1645 / 6 / 106
GOF on F^2	1.048	1.091
R_1, wR_2 [$F_o^2>2\sigma(F_o^2)$][a]	0.0327, 0.0869	0.0231, 0.0553
R_1, wR_2 (all data)[a]	0.0412, 0.0918	0.0286, 0.0570
Largest diff. peak and hole (e·Å^{-3})	1.926 and -1.843	1.811 and -1.526

[a] $R_1 = \Sigma||F_o| - |F_c||/\Sigma|F_o|$ and $wR_2 = [\Sigma w(F_o^2 - F_c^2)^2/ \Sigma w F_o^4]^{1/2}$ for $F_o^2 > 2\sigma(F_o^2)$.

Table S2. Atomic coordinates and equivalent isotropic displacement parameters for $Pb_6O_4(BO_3)(NO_3)$ and $Pb_6O_2(BO_3)_2(NO_3)F$. U(eq) is defined as one-third of the trace of the orthogonalized U_{ij} tensor.

	x	*y*	*z*	U(eq)	BVS
			$Pb_6O_4(BO_3)(NO_3)$		
Pb(1)	0.7500	0.5561(1)	0.8203(1)	0.036(1)	2.37
Pb(2)	0.2500	0.2500	0.8658(1)	0.036(1)	2.06
Pb(3)	0.7500	0.2500	0.6436(1)	0.035(1)	2.18
Pb(4)	0.2500	0.0127(1)	0.6192(1)	0.036(1)	2.13
N(1)	0.2500	0.7500	0.9140(30)	0.054(7)	5.37
B(1)	0.7500	0.7500	0.5690(30)	0.039(7)	2.86
O(1)	0.2500	0.6390(20)	0.9630(20)	0.100(7)	2.08
O(2)	0.2500	0.7500	0.8000(20)	0.080(9)	1.59
O(3)	1.0015(14)	0.3972(8)	0.7542(7)	0.032(2)	2.46
O(4)	0.7500	0.6199(15)	0.6294(14)	0.053(4)	1.84
O(5)	0.2500	0.02500	0.5512(17)	0.037(4)	2.19
			$Pb_6O_2(BO_3)_2(NO_3)F$		
Pb(1)	0.0585(1)	0.2500	0.4166(1)	0.027(1)	1.93
Pb(2)	0.4354(1)	0.0934(1)	0.2047(1)	0.028(1)	2.25
Pb(3)	0.6063(1)	0.2500	0.5953(1)	0.027(1)	1.75
Pb(4)	1.0895(1)	0.4069(1)	0.7974(1)	0.028(1)	2.24
N(1)	0.7494(15)	0.2500	0.0105(13)	0.040(3)	4.86
B(1)	0.7455(11)	-0.0015(8)	0.5038(12)	0.030(2)	3.00
F(1)	1.2805(15)	0.2500	0.9568(14)	0.079(3)	0.77
O(1)	0.7622(14)	0.3449(6)	-0.0549(10)	0.067(2)	1.81
O(2)	0.7154(13)	0.2500	0.1454(11)	0.044(2)	1.73
O(3)	0.6752(9)	0.0992(4)	0.4301(7)	0.033(1)	2.07
O(4)	0.7729(9)	-0.0991(4)	0.4226(7)	0.032(1)	2.09
O(5)	0.7925(8)	-0.0026(5)	0.6634(7)	0.037(1)	2.05
O(6)	0.3545(11)	0.2500	0.3113(10)	0.031(2)	2.42
O(7)	0.9586(10)	0.2500	0.6800(9)	0.024(2)	2.45

Table S3. Bond lengths [Å] and angles [deg] for $Pb_6O_4(BO_3)(NO_3)$ and $Pb_6O_2(BO_3)_2(NO_3)F$.

$Pb_6O_4(BO_3)(NO_3)$			
Pb(1)-O(3)	2.215(8)	N(1)-O(1)	1.19(3)
Pb(1)-O(3)#2	2.215(8)	N(1)-O(1)#9	1.19(3)
Pb(1)-O(4)	2.236(15)	N(1)-O(2)	1.28(4)
Pb(2)-O(3)#4	2.358(8)	B(1)-O(4)#1	1.41(2)
Pb(2)-O(3)#2	2.358(8)	B(1)-O(4)	1.41(2)
Pb(2)-O(3)#5	2.358(8)	B(1)-O(5)#10	1.35(4)
Pb(2)-O(3)#6	2.358(8)		
Pb(3)-O(3)#8	2.363(8)		
Pb(3)-O(3)	2.363(8)	O(1)-N(1)-O(1)#9	124.0(4)
Pb(3)-O(3)#5	2.363(8)	O(1)#9-N(1)-O(2)	118.1(19)
Pb(3)-O(3)#2	2.363(8)	O(1)-N(1)-O(2)	118.1(19)
Pb(4)-O(3)#5	2.254(8)	O(4)#1-B(1)-O(4)	122.0(3)
Pb(4)-O(3)#6	2.254(8)	O(5)#10-B(1)-O(4)#1	119.1(13)
Pb(4)-O(5)	2.372(6)	O(5)#10-B(1)-O(4)	119.1(13)

Symmetry transformations used to generate equivalent atoms:
#1) -x+3/2, -y+3/2, z; #2) -x+3/2, y, z; #3) -x+1/2, -y+1/2, z; #4) x-1, y, z; #5) -x+3/2, -y+1/2, z; #6) x-1, -y+1/2, z; #7) x+1, y, z; #8) x, -y+1/2, z; #9) -x+1/2, -y+3/2, z; #10) -x+1, -y+1, -z+1.

$Pb_6O_2(BO_3)_2(NO_3)F$			
Pb(1)-O(4)#1	2.390(6)	N(1)-O(1)	1.249(9)
Pb(1)-O(4)#2	2.390(6)	N(1)-O(1)#4	1.249(9)
Pb(1)-O(6)	2.387(7)	N(1)-O(2)	1.267(14)
Pb(1)-O(7)#3	2.570(8)	B(1)-O(3)	1.369(11)
Pb(2)-O(2)	2.750(7)	B(1)-O(4)	1.369(11)
Pb(2)-O(3)	2.316(6)	B(1)-O(5)	1.392(12)
Pb(2)-O(5)#1	2.369(5)		
Pb(2)-O(6)	2.159(4)		
Pb(3)-O(3)	2.381(6)	O(1)#4-N(1)-O(1)	122.0(12)
Pb(3)-O(3)#4	2.381(6)	O(1)#4-N(1)-O(2)	119.0(6)
Pb(3)-O(6)	2.751(9)	O(1)-N(1)-O(2)	119.0(6)
Pb(3)-O(7)	2.362(7)	O(3)-B(1)-O(5)	118.8(8)
Pb(4)-F(1)	2.493(6)	O(4)-B(1)-O(3)	120.9(8)
Pb(4)-O(4)#5	2.336(6)	O(4)-B(1)-O(5)	120.2(8)
Pb(4)-O(5)#4	2.395(6)		
Pb(4)-O(7)	2.184(4)		

Symmetry transformations used to generate equivalent atoms:
#1) -x+1, -y, -z+1; #2) -x+1, y+1/2, -z+1; #3) x-1, y, z; #4) x, -y+1/2, z; #5) -x+2, y+1/2, -z+1; #6) -x+2, y-1/2, -z+1; #7) x+1, y, z.

Table S4. Crystallographic data for inorganic compounds containing anion-centered $[OPb_4]$ tetrahedra and π-conjugated units.

compounds	space group	Structural feature	ref
$[Pb_4O]Pb_2(BO_3)_3Cl$	*Pbcm*	isolated $[OPb_4]$ tetrahedra + BO_3 units	6
$[Pb_4O]Pb_2(BO_3)_3F$	*Pbcm*	isolated $[OPb_4]$ tetrahedra + BO_3 units	7
$[Pb_4O]Pb_2(BO_3)_3Br$	*Pbcm*	isolated $[OPb_4]$ tetrahedra + BO_3 units	7
$Pb[Pb_4O](OH)_2(CO_3)$	$P6_3cm$	isolated $[OPb_4]$ tetrahedra + CO_3 units	8
$[Pb_8O_3](BO_3)_2(B_2O_5)$	*Aba*2	isolated $[O_3Pb_8]$ cluster + BO_3 units	9
$[Pb_{13}O_8](OH)_6(NO_3)_4$	$R\bar{3}$	isolated $[O_8Pb_{13}]$ cluster + NO_3 units	10
$Pb_6O_2(BO_3)_3(SO_4)$	*Pnma*	$[O_2Pb_6]$ chain + BO_3 units	11
$Pb_6O_2(BO_3)_3(MoO_4)$	*Cmcm*	$[O_2Pb_6]$ chain + BO_3 units	12
$Pb_6O_2(BO_3)_3(CrO_4)$	*Pnma*	$[O_2Pb_6]$ chain + BO_3 units	12
$[Pb_3O_2](CO_3)$	*Pnma*	$[O_2Pb_3]$ chain + CO_3 units	13
$[Pb_3O_2]_2(OH)(NO_3)(CO_3)$	*Pnma*	$[O_2Pb_3]$ chain + CO_3/NO_3 units	14
$[Pb_3O_2](OH)(NO_3)$	$Pca2_1$	$[O_2Pb_3]$ chain + NO_3 units	15
$Pb_2(O_4Pb_8)(BO_3)_3Br_3$	*C*2/*c*	$[OPb_2]$ chain + BO_3 units	16
$Pb_2(O_8Pb_{12})(BO_3)_2Br_6$	*C*2/*c*	$[O_2Pb_3]$ ribbon + BO_3 units	16
$[O_2Pb_3]_2(BO_3)Br$	*Cmcm*	$[O_2Pb_3]$ double chain + BO_3 units	17
$Pb_{47}O_{24}(OH)_{13}Cl_{25}(BO_3)_2(CO_3)$	*Cm*	$[Pb_{44}O_{24}(OH)_{12}]$ layer + BO_3/CO_3 units	18
$Pb_6O_4(BO_3)(NO_3)$	*Pmmn*	$[O_4Pb_6]$ double chain + BO_3/NO_3 units	This work
$Pb_6O_2(BO_3)_2(NO_3)F$	$P2_1/m$	$[O_2Pb_6]$ chain + BO_3/NO_3 units	This work

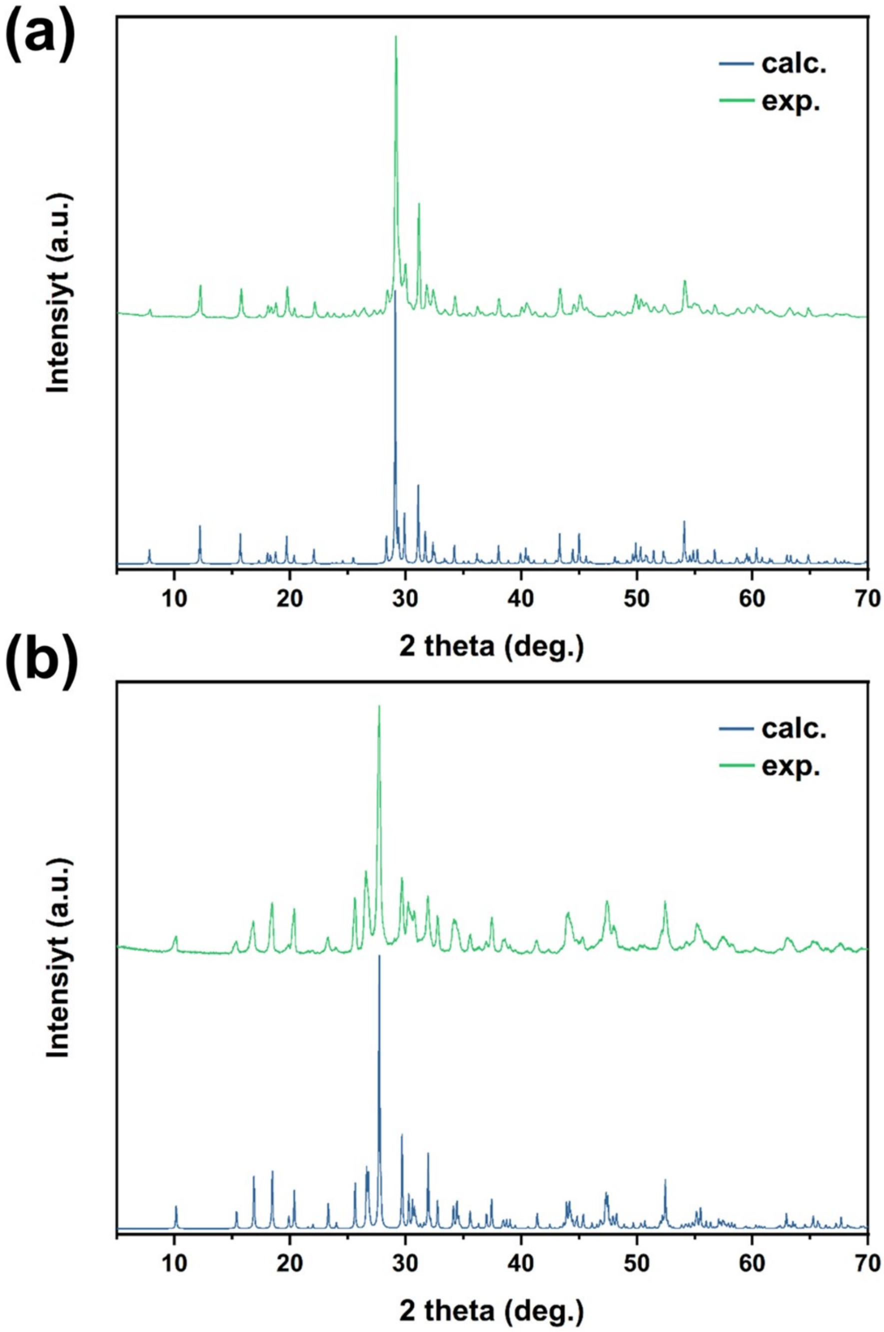

Figure S1. The calculated and experimental powder XRD patterns of (a) $Pb_6O_4(BO_3)(NO_3)$ and (b) $Pb_6O_2(BO_3)_2(NO_3)F$.

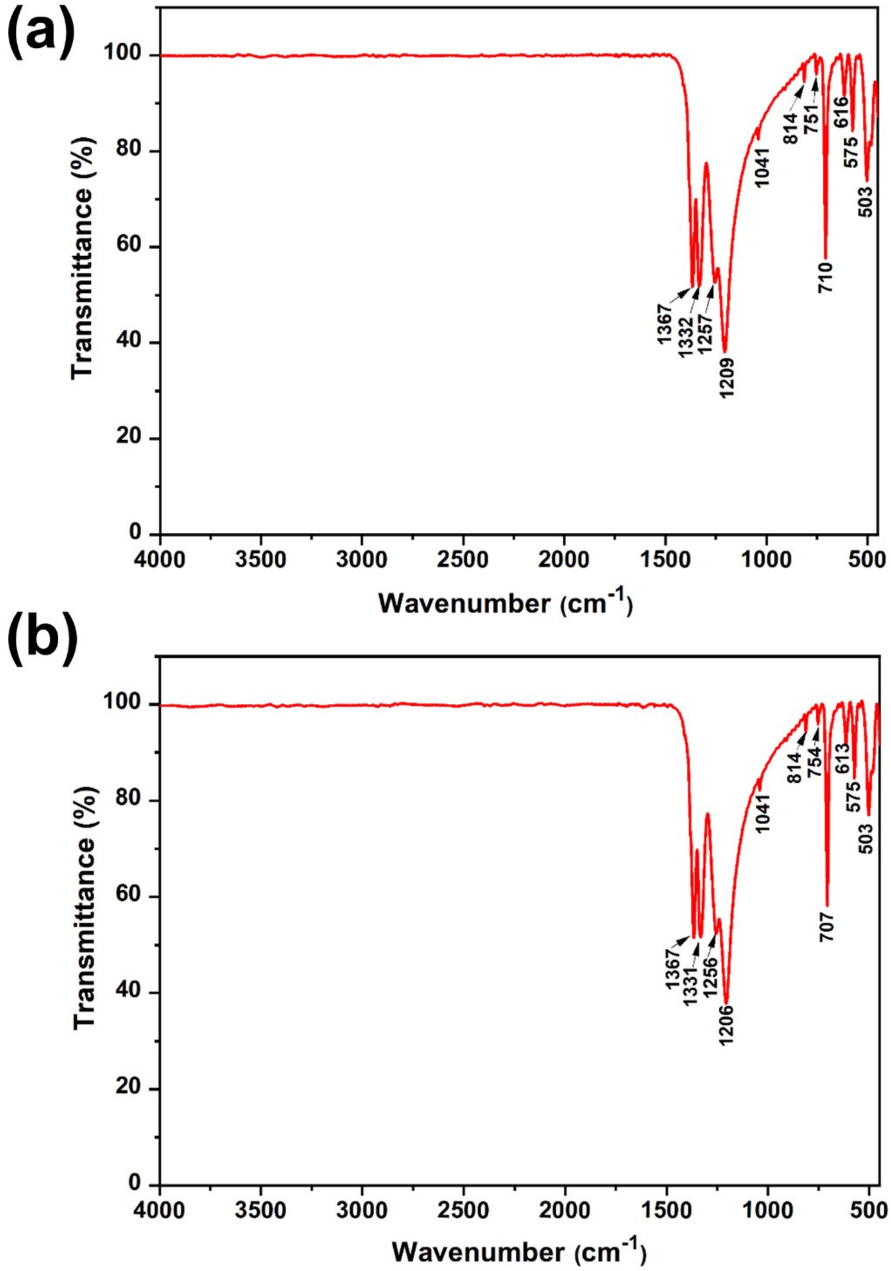

Figure S2. The IR spectra of (a) $Pb_6O_4(BO_3)(NO_3)$ and (b) $Pb_6O_2(BO_3)_2(NO_3)F$.

.

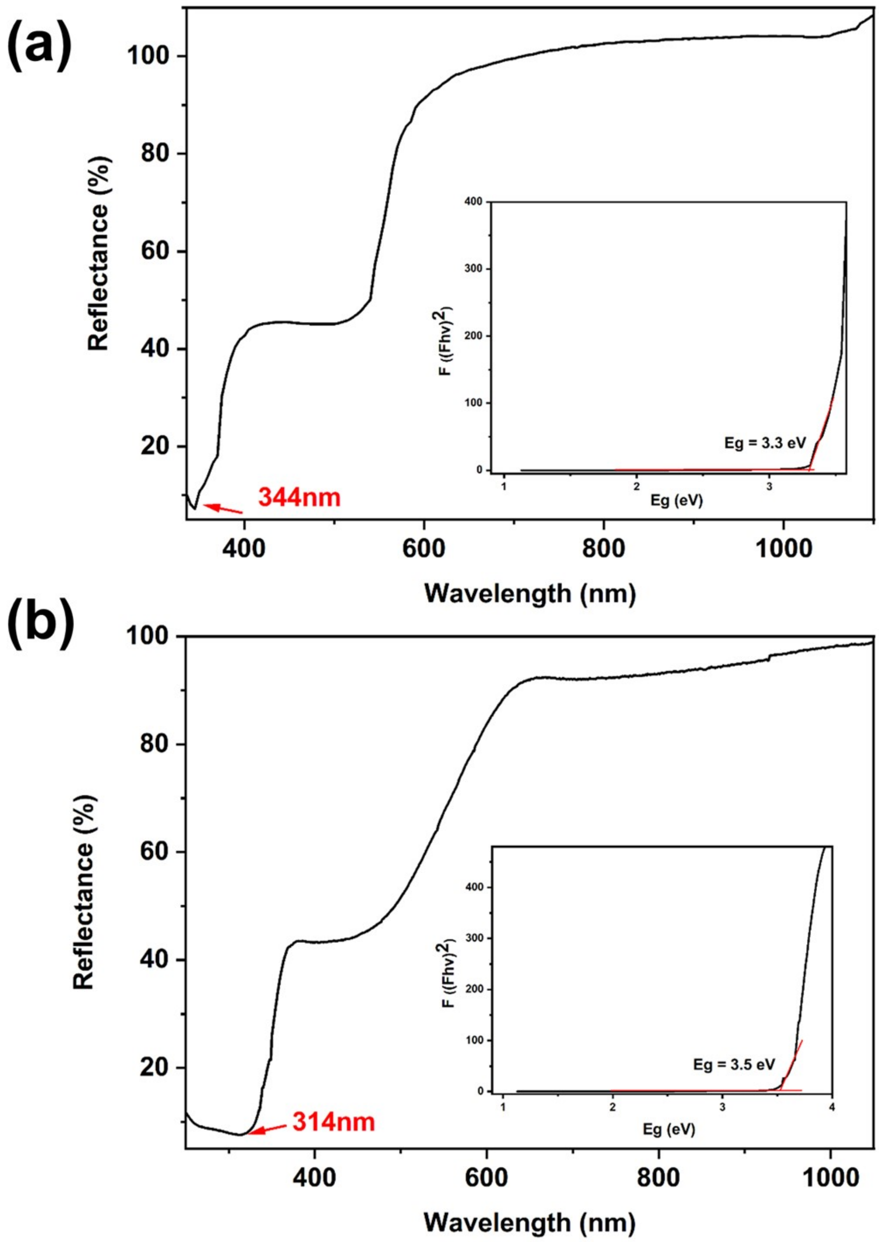

Figure S3. The UV−Vis−NIR diffuse reflectance spectra of (a) $Pb_6O_4(BO_3)(NO_3)$ and (b) $Pb_6O_2(BO_3)_2(NO_3)F$.

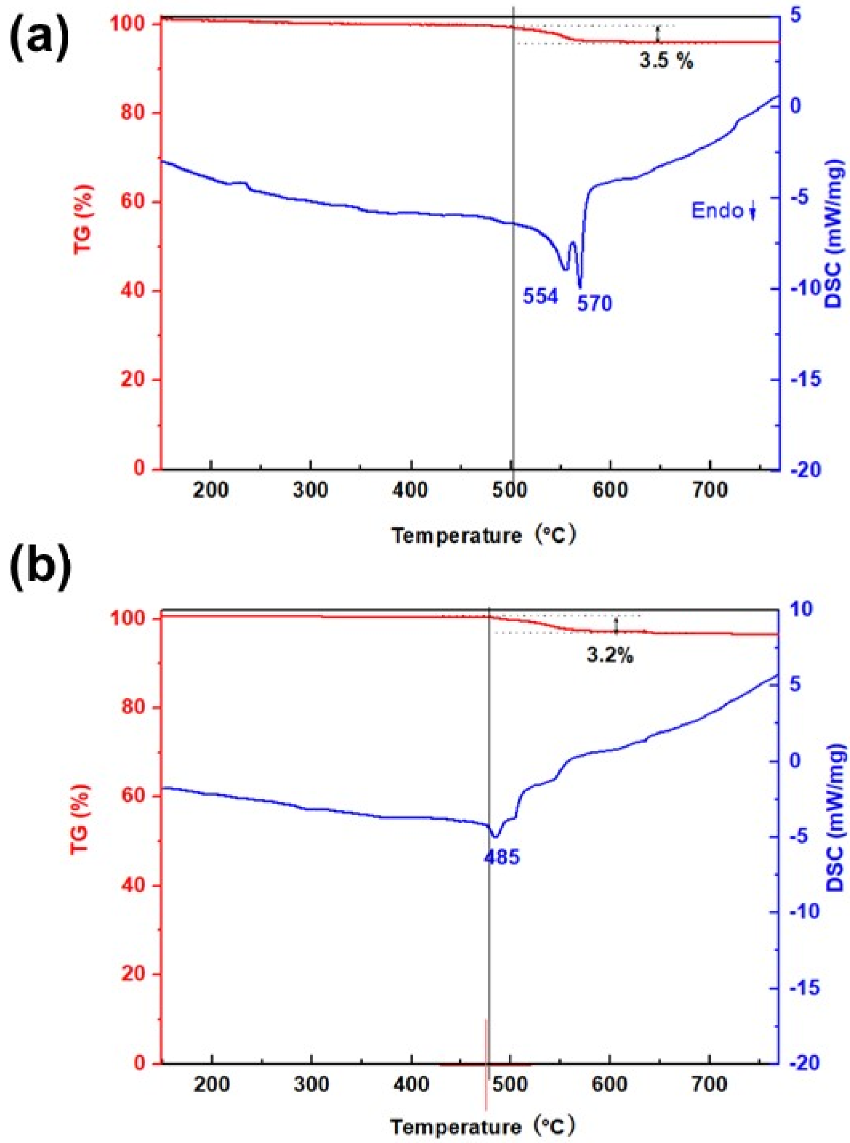

Figure S4. The TG and DSC curves of (a) $Pb_6O_4(BO_3)(NO_3)$ and (b) $Pb_6O_2(BO_3)_2(NO_3)F$.

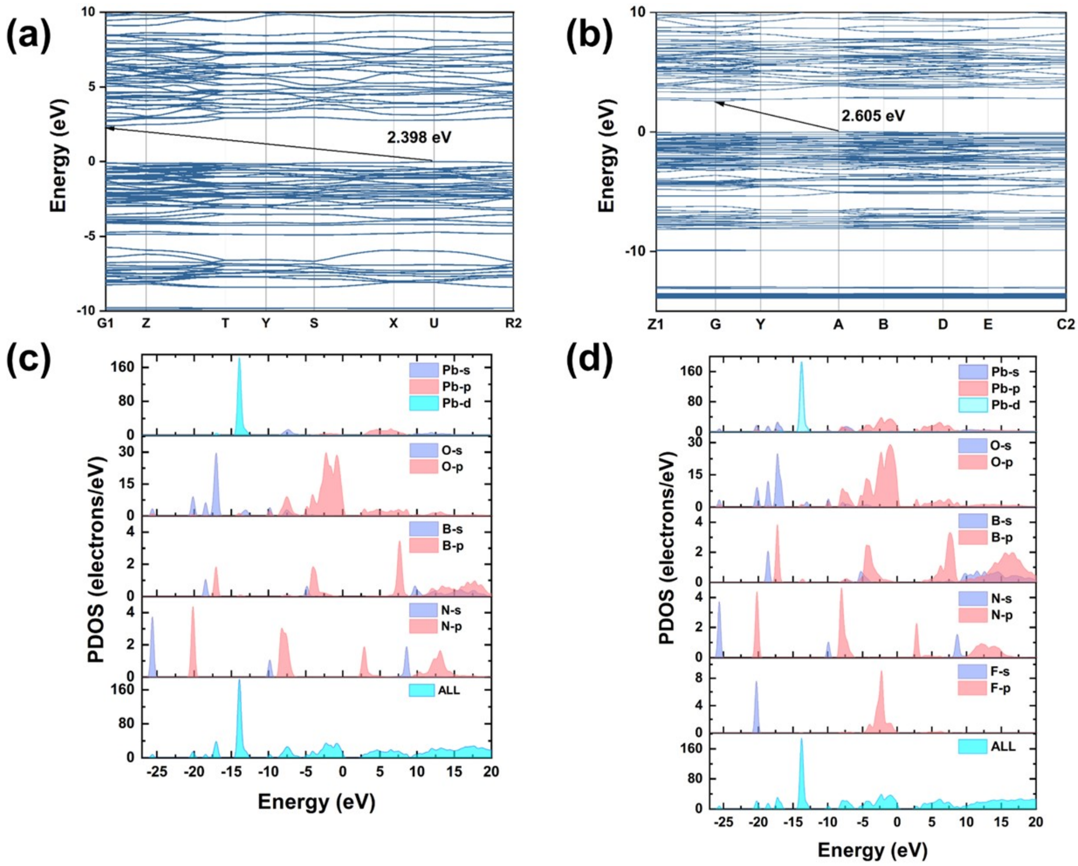

Figure S5. The bandgap of (a) $Pb_6O_4(BO_3)(NO_3)$ and (b) $Pb_6O_2(BO_3)_2(NO_3)F$. The PDOS of (c) $Pb_6O_4(BO_3)(NO_3)$ and (d) $Pb_6O_2(BO_3)_2(NO_3)F$.

Reference

1. SAINT, *Version 7.60A, Bruker analytical X-ray Instruments, inc.,Madison, WI, 2008*.
2. O. V. Dolomanov, L. J. Bourhis, R. J. Gildea, J. A. K. Howard and H. Puschmann, *J. Appl. Cryst.* , 2009, **42**, 339–341.
3. S. J. Clark, M. D. Segall, C. J. Pickard, P. J. Hasnip, M. I. J. Probert, K. Refson and M. C. Payne, *Z. Kristallogr.*, 2005, **220**, 567−570.
4. J. S. Lin, A. Qteish, M. C. Payne and V. Heine, *Phys. Rev. B*, 1993, **47**, 4174–4180.
5. A. M. Rappe, K. M. Rabe, E. Kaxiras and J. D. Joannopoulos, *Phys. Rev. B*, 1990, **41**, 1227–1230.
6. H. Behm, *Acta Cryst. C*, 1983, **39**, 1317-1319.
7. L. Y. Dong, S. L. Pan, H. P. Wu, X. Su, H. W. Yu, Y. Wang, Z. H. Chen, Z. J. Huang and Z. H. Yang, *J. Solid State Chem.*, 2013, **204**, 64-69.
8. S. V. Krivovichev and P. C. Burns, *Mineral. Mag.*, 2000, **64**, 1069-1075.
9. H. W. Yu, S. L. Pan, H. P. Wu, W. W. Zhao, F. F. Zhang, H. Y. Li and Z. H. Yang, *J. Mater. Chem.*, 2012, **22**, 2105-2110.
10. Y. Li, S. V. Krivovichev and P. C. Burns, *J. Solid State Chem.*, 2001, **158**, 74-77.
11. B. Aurivillius, *Chem. Scr.*, 1983, **22**, 168-170.
12. X. A. Chen, F. P. Song, X. N. Chang, H. G. Zang and W. Q. Xiao, *J. Solid State Chem.*, 2009, **182**, 3091-3097.
13. S. V. Krivovichev and P. C. Burns, *Mineral. Mag.*, 2000, **64**, 1077-1087.
14. Y. Li, S. V. Krivovichev and P. C. Burns, *J. Solid State Chem.*, 2000, **153**, 365-370.
15. S. V. Krivovichev, Y. Li and P. C. Burns, *J. Solid State Chem.*, 2001, **158**, 78-81.
16. L. Y. Dong, S. L. Pan, Y. Wang, H. W. Yu, X. Y. Dong, S. J. Han and M. Zhang, *Inorg. Chem.*, 2013, **52**, 11377-11384.
17. L. Y. Dong, J. Yang, S. G. Shen, Z. Z. Liu, X. J. Chen and S. F. Sun, *Z. Anorg. Allg. Chem.*, 2017, **643**, 471-476.
18. S. V. Krivovichev, R. Turner, M. Rumsey, O. I. Sidra and C. A. Kirk, *Mineral. Mag.*, 2009, **73**, 103-117.